

A New Prognostics Approach for Bearing based on Entropy Decrease and Comparison with existing Methods

Seokgoo Kim¹, Sungho Park², Ju-Won Kim³, Junghwa Han³, Dawn An⁴, Nam Ho Kim⁴, Joo-Ho Choi⁵

^{1,2}*Dept. of Aerospace and Mechanical Engineering, Korea Aerospace University, Goyang-City, Gyeonggi-do Korea*

*sgkim@kau.kr
shpark6386@nate.com*

³*Korea railroad corporation, Daejeon, Korea*

*pazazatj@korail.com
argun@korail.com*

⁴*Mechanical & Aerospace Eng. University of Florida, Gainesville, FL, USA*

*dawnan@udf.edu
nkim@udf.edu*

⁵*School of Aerospace and Mechanical Engineering, Korea Aerospace University, Goyang-City, Gyeonggi-do Korea*

jhchoi@kau.ac.kr

ABSTRACT

In this paper, a new method is proposed for the bearing prognosis based on the energy entropy, in which the normalized energy in the frequency spectrum is calculated over the cycles, frequency band is selected that shows greater decrease relative to the others, and entropy is computed as a trending feature. As opposed to the traditional features, which exhibit noisy fluctuation, non-monotonic change or only an abrupt increase near the end of life, the proposed energy entropy shows the smooth and constant decrease over the cycles which may represent the degree of fault progression. In order to illustrate the advantage, four traditional features - RMS, kurtosis, MAS kurtosis and envelope and the new feature - energy entropy are examined and compared using the three cases of bearing data named FEMTO, IMS and LOCAL, all from the bearing life test.

1. INTRODUCTION

Bearing is one of the most important components in rotating machineries because it can cause catastrophic failure in the whole system when not maintained properly. In order to prevent failures while extending its use over the bearing's life, many researches have been made under the name of prognostics and health management (PHM), which includes

the data acquisition from the sensor, feature extraction via signal processing, and fault diagnosis or failure prognosis to aid decision on the maintenance action. Many review articles are available that have addressed the state-of-the-art of the related techniques, among which some representative ones are given in (Lebold et al. 2000, Jardine 2016, Heng et al. 2009, Lee et al. 2014). To date, most of the studies have been made for the diagnostics that estimates the fault severity at the current time of operation, which is useful for immediate interruption to avoid failures. On the other hand, prognostics literature is much smaller, which is to predict how soon the failure will take place under the future operation, which requires the modeling of fault progression and inherent uncertainty for long-term prediction. Compared to the diagnostics, the prognostics provides much more advantage that it allows operation to its full end of life while enabling the maintenance readiness in advance. In this sense, the prognostics is a new promising area, which has to be explored with more depth.

In the bearing prognostics, the most common practice is to employ vibration sensor that measures the acceleration. The challenge of this method is that the raw sensor data are not consistent in terms of their degradation pattern and the end-of-lives, even if they are from the identical bearings and operating conditions. Also, they rarely exhibit degradation information in its apparent form except near the end of life. Therefore, many studies have been devoted to find out proper features that can identify the incipient fault and monitor the trend over time as the fault develops. Traditionally, the

Seokgoo Kim et al. This is an open-access article distributed under the terms of the Creative Commons Attribution 3.0 United States License, which permits unrestricted use, distribution, and reproduction in any medium, provided the original author and source are credited.

features have been classified into two groups: time domain and frequency domain features. Among these, the traditional features that are often used in the literature are the root mean square (RMS) and the kurtosis in the time domain, and the spectral kurtosis and envelope analysis in the frequency domain (Yan et al., 2008 & Siegel et al., 2011). Siegel et al (2011) studied prognostics of helicopter oil-cooler bearing by extracting and trending these features using the data provided by Impact Technologies. Sutrisno et al (2012) and Wang et al (2012) have studied the FEMTO experimental data for the IEEE 2012 PHM data challenge competition, in which the Moving Average Spectral (MAS) kurtosis and envelope analysis were applied respectively.

Siew et.al (2015) used the data from Bearing Prognostics Simulator provided by SpectraQuest, to study fault trending using the RMS, kurtosis and envelope parameters. Randall et al (2011) has addressed in his tutorial paper the detail of several essential techniques necessary to the majority of bearing diagnostics, which includes the spectral kurtosis and envelope analysis. He also applied the techniques to the three cases ranging from high speed bearing for turbine engine to the low speed main bearing on a radar tower. The results in these studies have shown valuable indication that the features can represent the fault severity with reasonable degree. However, they have some limitations that make the features less useful from the prognostic perspectives. The features fluctuate substantially over time even after the signal denoising or do not show a distinct pattern of degradation which lack the monotonicity in their change over the cycles or show only the abrupt increase near the end of life. All these aspects render the features difficult to apply to the prognostics.

In order to overcome this problem, the authors (An et al., 2016) have recently proposed a new method using the entropy decrease which is more suitable for the purpose of prognostics. The idea is based on the observation that the entropy decreases at certain specific frequencies as the fault progresses. As a result of implementation, we have found that the entropy feature shows substantial and smooth decrease from the early stage of the fault progression. The disadvantage is that it is empirical with little physical understanding. In this study, an enhanced version is presented which shows better performance and provides more physical interpretation. The final aim of the prognosis is to predict the remaining useful life (RUL) using the degradation trend until the specified threshold is reached. This is however not addressed in this study. Instead, we focus only on investigating the best feature in view of prognostic performance. To this end, three cases of the bearing experiments are considered, which are the FEMTO data used in (Sutrisno et al., 2012 & Wang et al., 2012), IMS data used in (Qiu et al., 2006 & Caesarendra et al., 2010), and the data from local manufacturer which was made during their accelerated life tests. For these data, four existing features: RMS, kurtosis, MAS kurtosis and envelope peaks at the fault frequencies are examined, trended over cycles and compared

with the authors' entropy method to evaluate the performance of one over the others.

2. DATA SET DESCRIPTION

In this section, three cases of the bearing experimental data are described, which are designated as the FEMTO given from the PHM conference competition in 2012, the IMS in the prognostic data repository by NASA Ames research center and the LOCAL from a manufacturer in Korea. Note that all of the data are made from the life tests with constant speed and loadings conducted in the lab instead of the real field operations. Therefore, there is less need to address other considerations such as the denoising, order tracking or time synchronous averaging to remove influence from the other components frequency or the fluctuating speeds. The life duration of FEMTO and LOCAL are very short because they are made from accelerated tests whereas the IMS data is long extending to 30-40 days, which means that the load is normal.

2.1. FEMTO data

More detail explanation of FEMTO data and experimental configuration is given in the Figure 1. Vibration signals are monitored under the radial load given in horizontal direction from the two sensors in horizontal and vertical directions. Raw data are taken during 0.1 second with 25.6 kHz at every 10 seconds, which produces 2560 samples in each cycle. Operating conditions and number of data are listed in Table 1. Two data sets are made under three different operating conditions respectively. Based on the raw signals, failure is assumed when the vertical acceleration reaches 20g.

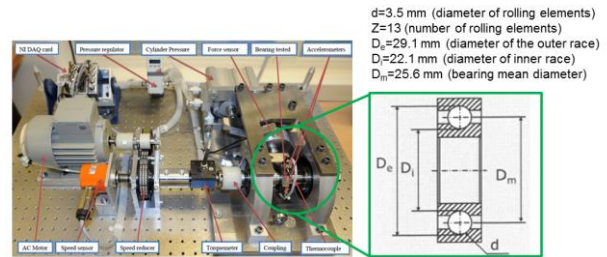


Figure 1. Experimentation platform

Table 1. Experimental condition

| | Radial force | Rotating speed |
|-------------|--------------|----------------|
| Condition 1 | 4000 N | 1800 rpm |
| Condition 2 | 4200 N | 1650 rpm |
| Condition 3 | 5000 N | 1500 rpm |

2.2. IMS data

The data can be downloaded from 'Bearing Data Set', IMS, University of Cincinnati NASA Ames Prognostics Data Repository. They were used for the study in (Qiu et al 2006

& Caesarendra et al. 2010). Four double row bearings (16 rollers) are installed on a shaft as shown in Figure 2, and the rotating speed and radial load are, respectively, 2000 RPM and 6000 lbs. Three sets are made from the repeated experiment under this condition. Vibration data was collected every 20 minutes with sampling rate 20kHz and the data length was 20,480points. The test was carried out for 35 days until a significant amount of metal debris was found on the magnetic plug of the test bearing.

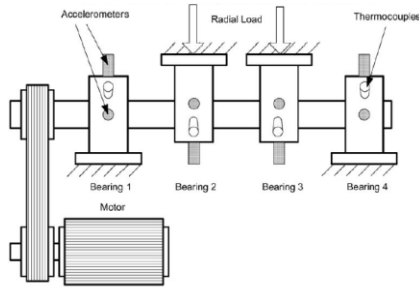


Figure 2. Bearing test rig

2.3. LOCAL data

Under the combined loads with radial and thrust being 617 and 370 kgf, the bearings are operated with 1000 rpm until the acceleration level reaches a certain predetermined value. The bearing and installed sensor are shown in Figure 3. Three and one data set are collected with 8 kHz and 32 kHz sampling rate respectively. In all the failed bearings, the failure modes are spalling of balls inboard in common. As expected, the failure time varies significantly from 3.5 to 11.2 hours, despite the identical bearings under the same loading condition.

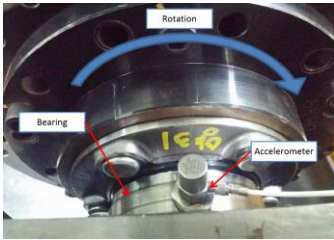


Figure 3. Bearing test rig and installed sensor

3. EXISTING APPROACHES FOR PROGNOSTIC FEATURES

Before extraction of time domain features, the raw data go through a smoothing process by exponential filter with factor $\alpha = 0.9$ (Wang 2012). Then the time series RMS and kurtosis at each cycle are calculated as follows.

$$RMS = \sqrt{\frac{1}{N} \sum_{i=1}^N x_i^2} \quad (1)$$

$$Kurtosis = \frac{\frac{1}{N} \sum_{i=1}^N (x_i - \bar{x})^4}{\sigma^4} \quad (2)$$

The method for MAS kurtosis is explained in (Sutrisno et al. 2012). At first, time series kurtosis is obtained using a band pass filtered signal over a given frequency range. Then moving average filter is applied with a specific window size to the results and trend the value over time. The monotonicity of the increasing trend is quantified by Spearman's rank correlation coefficient between the MAS kurtosis and time. If the value is close to 1, it represents perfect monotonic increase over time. To maximize the monotonicity of the trend, the frequency range is divided by a small interval over the spectrum, coefficient is calculated at every interval, and determine the optimum range that maximizes the coefficient. It should be noted that the spectral kurtosis mentioned here is different from those addressed in the literature (Randall 2011). The word "spectral" may have been assigned due to the band pass filtering of the raw signal, which is however not the same approach.

The envelope analysis is explained in (Randall 2011, McInerney 2003). This method was developed more than 30 years ago and is now used as a benchmark method. The procedure is that the raw signal is band pass filtered in a high frequency band in which the fault impulses are amplified by structural resonances. It is then amplitude demodulated to form the envelope signal using the Hilbert transform. The final step is the spectrum analysis of the envelope signal to extract the desired diagnostic information at the bearing fault frequencies (ball pass frequency, spin frequency and so on) and its harmonics. The drawback of the envelope analysis is the difficulty in the frequency band selection, which is one of the most critical steps that can have a large influence on the results. Among the many criteria suggested for this, the band chosen previously from the MAS kurtosis study is used for the envelope analysis.

4. NEW APPROACH USING ENTROPY

Recently, the authors have developed a new approach based on the entropy decrease at specific frequencies. While the details are given in (An 2016), the process is briefly summarized here for convenience. The steps are illustrated in Figure 4, and is summarized as follows.

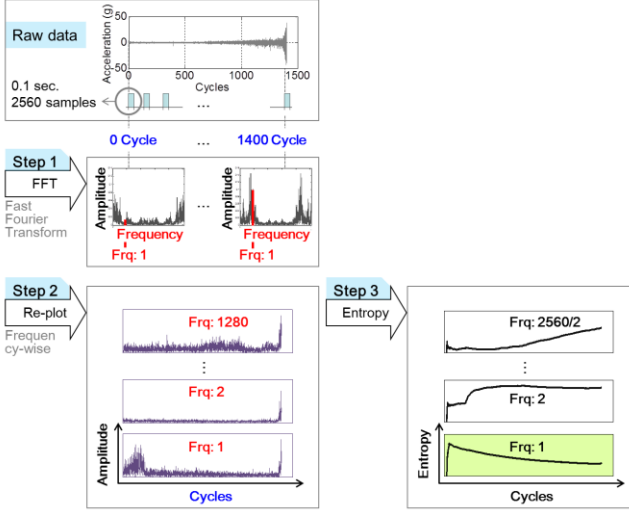


Figure 4. Procedure of entropy feature extraction

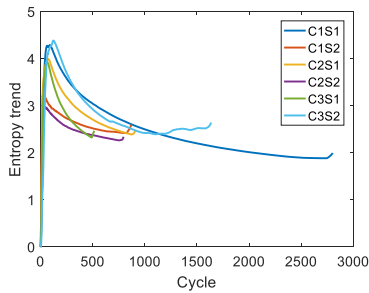
Step 1: Convert the raw data in time domain at each cycle into frequency domain using FFT to get the amplitudes as a function of frequency.

Step 2: Reshape the FFT results frequency-wise. That is, the amplitude change is given in terms of cycles at each frequency (e.g., Frq: 1), which is called frequency-wise plot here.

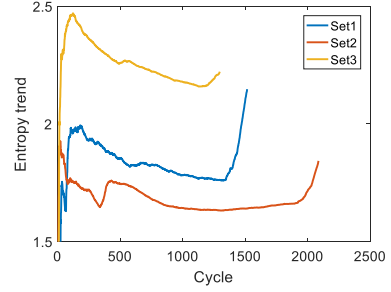
Step 3: Calculate entropy using the following equation and select specific frequencies showing entropy decrease (e.g., Frq: 1) among the results over the entire frequencies.

$$H(X) = -\sum_{i=1}^n p(x_i) \log_2 p(x_i) \quad (3)$$

Among the several frequencies with entropy decrease, those with biggest decrease are selected, average is taken, and this is used as the feature. The results by this method for the FEMTO data are given in Figure 5(a), in which the curve exhibits smooth and gradual degradation. The uniqueness of this method is in this behavior, which the authors believe that it may represent the fault progression introduced from the early stage of the cycles. If we can set a proper threshold for the failure to this, the RUL can be predicted with much more clarity than the traditional methods.



(a) FEMTO data



(b) LOCAL data with 8kHz sampling rate

Figure 5. Original entropy for the two cases: FEMTO and LOCAL data

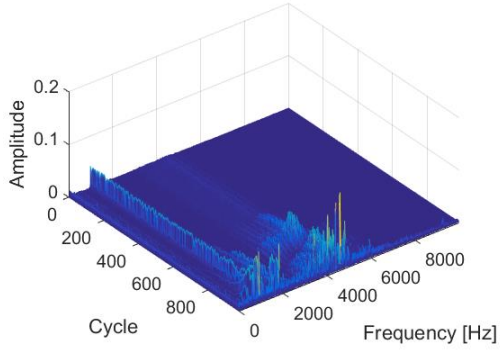
The method, however, lacks the physical interpretation about why this represents the fault progression. Besides, it has failed to show the monotonic degradation for the other cases, as shown in Figure 5(b) for the LOCAL data with 8K sampling rate. To overcome this, an enhanced version is developed in this study, which shows better performance and enables more physical interpretation. The procedure is outlined as follows.

Step 1: Convert the raw data in time domain at each cycle into frequency domain using FFT, and calculate the energy as in the following equation. Then draw the 3-D plot with the height being the energy magnitude at the domain of cycle versus frequency. This is shown in Figure 6(a) for the IMS data set 2, bearing 1.

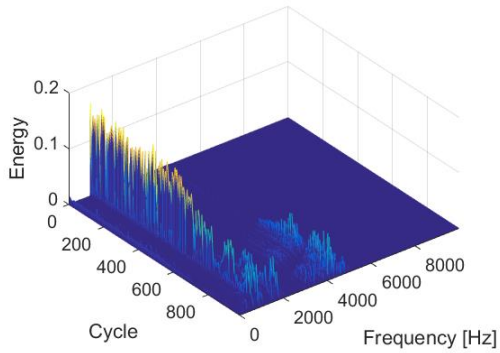
$$E_f = A_f^2 \sum_{F>0} A_F^2 \quad (4)$$

Step 2: Select frequency band which includes the maximum value at the initial stage, which is around 1000 Hz in the figure. The reason to select this is because the normalized energy at this frequency band at the initially state is reduced because the energy value grows at the other frequency regions due to the fault creation and progression. This is evidenced in Figure 6(b), which shows the constant behavior at the initially normal state until the 600 cycles, followed by the energy increase at the other regions 3000~6000 Hz. Due to this, the normalized energy at 1000 Hz is reduced, which represents the degree of fault progression.

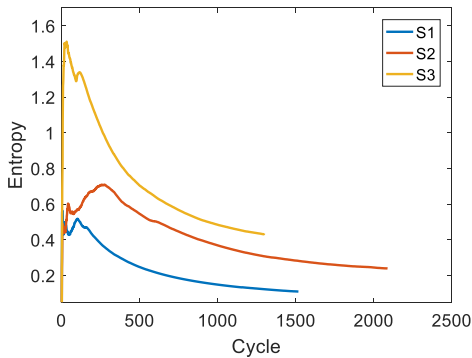
Step 3: Calculate entropies at the selected frequency band as suggested by Step 2, make average and use it as the feature. In the Figure 6(c), the feature curve is shown again for the LOCAL data with 8K sampling rate, which exhibits the behavior of monotonic decrease.



(a) Amplitude trend of IMS data (Set2, Bearing1)



(b) Energy trend of IMS data (Set2, Bearing1)



(c) Energy entropy (LOCAL data)

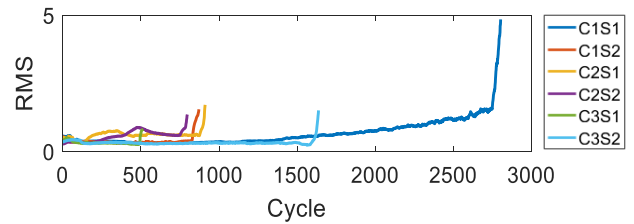
Figure 6. Process of entropy extraction from energy trend

5. RESULTS AND DISCUSSIONS

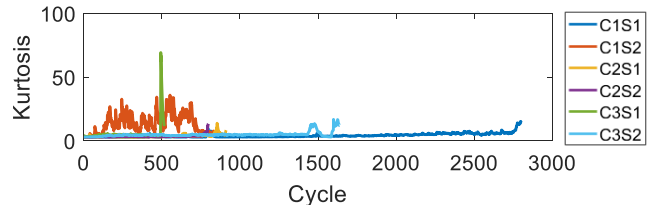
In order to examine the performance of four traditional features and the entropy of our method quantitatively from prognostics viewpoint, Spearman's rank correlation coefficient mentioned earlier is employed. Note that the values of all the traditional feature unanimously increase whereas the entropy of our method decreases as a measure of fault progression. The higher absolute value represents the superior performance showing more monotonic degradation (increase or decrease) behavior over time.

5.1. FEMTO data

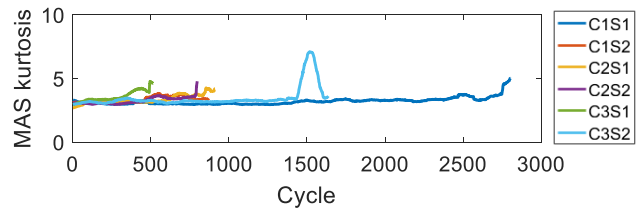
For the FEMTO data, trending curves are plotted for the first three features – RMS, kurtosis and MAS kurtosis, in which the six curves are given for the two data sets from three different conditions as was defined in Table 1. In case of MAS kurtosis, the whole spectrum of 0~12.8kHz is divided by the interval of 500 Hz and find out the range 5500-6000 Hz is the best. This is used for the MAS kurtosis and envelope study. The correlation coefficient values are also given in Table 2. As can be seen, the features severely fluctuate (C1S2 (Condition 1, Set 2) in kurtosis for example) even after the exponential smoothing to cancel the noise, do not show monotonicity (C2S2 in RMS for example) or increase abruptly only near the end (C3S2 in MAS kurtosis), which make it hard to make prediction model for prognosis. In the Table 2, the coefficient value of C3S1 in MAS kurtosis show the best value of 0.9570, which is however not so in practice. Therefore, another metric should be introduced in addition in the future to complement the drawback of coefficient evaluation.



(a) RMS trend



(b) Kurtosis trend



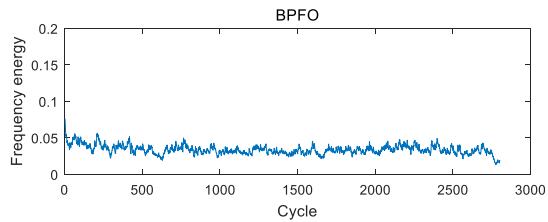
(c) Moving average spectral kurtosis

Figure 7. Feature trends of FEMTO data

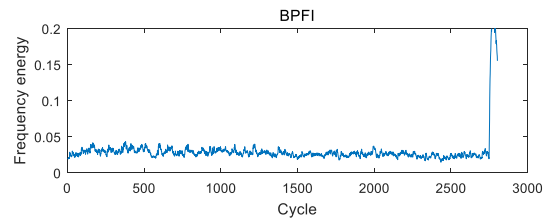
Table 2. Spearman’s rank correlation coefficient of FEMTO

| | RMS | Kurtosis | MAS kurtosis |
|------|---------|----------|--------------|
| C1S1 | 0.8638 | 0.9111 | 0.7747 |
| C1S2 | -0.0226 | 0.1334 | 0.8005 |
| C2S1 | 0.3428 | 0.7087 | 0.8473 |
| C2S2 | 0.7998 | 0.8669 | 0.8162 |
| C3S1 | -0.6021 | 0.3974 | 0.9570 |
| C3S2 | -0.1878 | 0.6039 | 0.6676 |

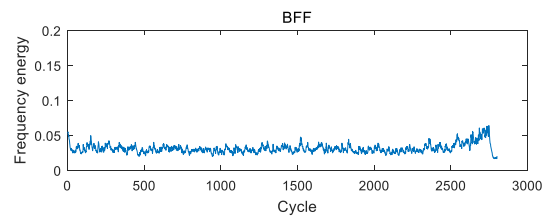
In case of envelope, there are four fault frequencies based on bearing dimension to keep track of as a measure of fault severity, and the results are in Figure 8. Since the inclusion of all the data set may make the figure more complex, only the ones with the best trend, i.e., the highest coefficient value, are given here. Likewise, the features show the same trend as above.



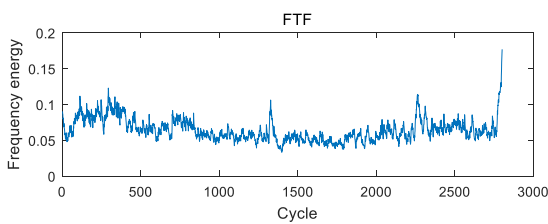
(a) Frequency energy trend of BPFO



(b) Frequency energy trend of BPFI



(c) Frequency energy trend of BFF



(d) Frequency energy trend of FTF

Figure 8. Envelope analysis of C1S1

In Figure 9, the result of energy entropy proposed in this study is plotted and the coefficient values given in table 3. As opposed to the traditional features, the curves show smooth and gradual but remarkable degrading behavior, which may be useful for the prognostics.

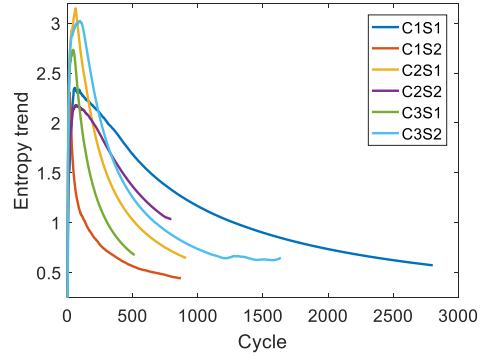


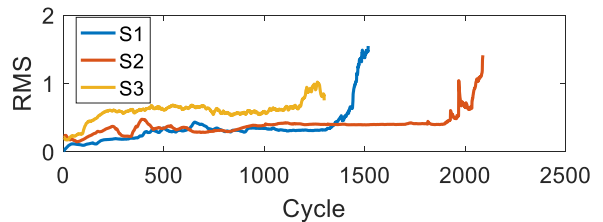
Figure 9. Energy entropy

Table 3. Spearman’s rank correlation of energy entropy of FEMTO

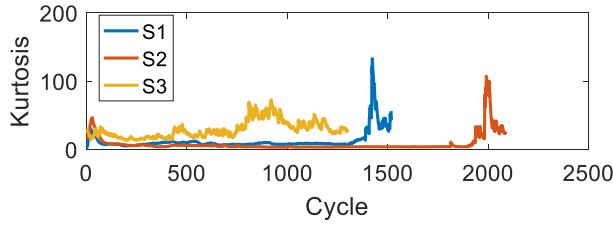
| | Entropy trend |
|------|---------------|
| C1S1 | -0.9924 |
| C1S2 | -0.9924 |
| C2S1 | -0.9863 |
| C2S2 | -0.9365 |
| C3S1 | -0.9723 |
| C3S2 | -0.9867 |

5.2. LOCAL data

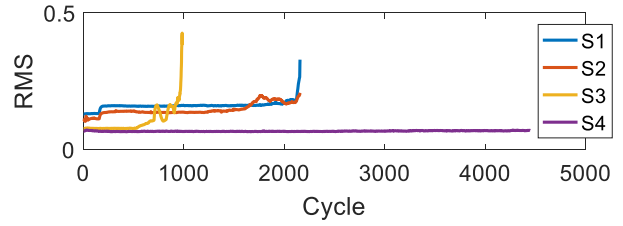
Three sets are examined which are from the 8K sampling rate. The frequency band for the MAS kurtosis and envelope analysis is 2200-2300 Hz in this case. Results for the RMS, kurtosis, MAS kurtosis and energy entropy are given in Figure 10 and Table 4. The similar behavior is observed in the LOCAL data too. For the envelope analysis, the result is not presented here since the similar behaviors to the FEMTO are observed.



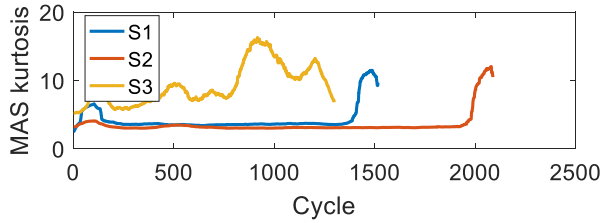
(a) RMS trend



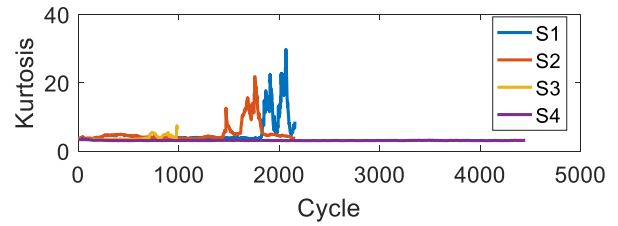
(b) Kurtosis trend



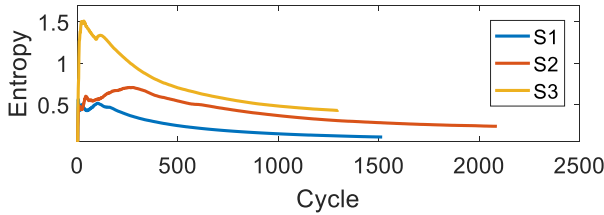
(a) RMS trend



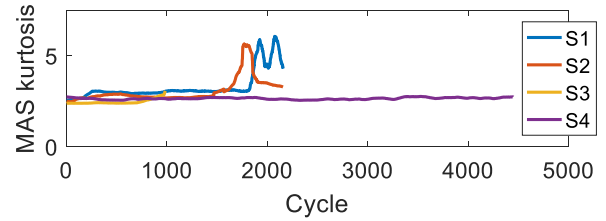
(c) Moving average spectral kurtosis trend



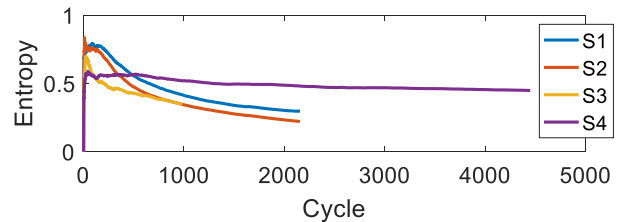
(b) Kurtosis trend



(d) Energy entropy trend



(c) Moving average spectral kurtosis



(d) Energy entropy trend

Figure 10. Feature trends of LOCAL data

Table 4. Spearman's rank correlation coefficient of LOCAL

| | RMS | Kurtosis | MAS kurtosis | Entropy |
|----|--------|----------|--------------|---------|
| S1 | 0.8013 | 0.3050 | 0.1721 | -0.9939 |
| S2 | 0.8044 | -0.2461 | 0.1021 | -0.9727 |
| S3 | 0.5385 | 0.6867 | 0.7859 | -0.9864 |

5.3. IMS data

Among the three sets of data for one condition, which includes the data from two accelerometers, four bearings, the set 1 for the bearing 3,4, set 2 for the bearing 1, and set 3 for the bearing 3 are chosen to illustrate the result because they have reached failure whereas the others did not. The frequency band for the MAS kurtosis and envelope analysis is 1000-1500 Hz in this case. Results for the RMS, kurtosis, MAS kurtosis and energy entropy are given in Figure 11 and

Table 5. The similar behavior is observed in the LOCAL data too. For the envelope analysis, the result is omitted for brevity. Set 1 for the bearing 3 : S1, set 1 for the bearing 4 : S2, set 2 for the bearing 1 : S3, and set 3 for the bearing 3 : S4.

Figure 11. Feature trends of IMS data

Table 5. Spearman's rank correlation coefficient of IMS

| | RMS | Kurtosis | MAS kurtosis | Entropy |
|----|--------|----------|--------------|---------|
| S1 | 0.8852 | 0.8940 | 0.8456 | -0.9953 |
| S2 | 0.8050 | 0.3695 | 0.6823 | -0.9961 |
| S3 | 0.8377 | 0.5982 | 0.8464 | -0.9716 |
| S4 | 0.6849 | -0.1191 | 0.3283 | -0.9837 |

As found in the several case studies, the traditional features have shown the undesirable behaviors such as the fluctuation, non-monotonicity or abrupt increase at the end. On the other hand, the energy entropy has shown the unique degradation

behavior with smoothness and monotonic decrease for all the test cases, which is much more useful for prognostic feature. Once the feature is chosen and trended with confidence, the remaining step is to set a threshold using the feature. This is however another challenge to be solved in the future study. Also the method should work well in the real field application which involves much greater noise with intervening components and variable operating conditions.

6. CONCLUSIONS

In this study, new feature, energy entropy, is introduced for the purpose of prognostics, and compared against the several traditional features available in the literature, which are the RMS and kurtosis in the time domain and the MAS kurtosis and envelope in the frequency domain. As found in the three case studies using FEMTO, IMS and LOCAL, all the results showed the same conclusion: the traditional features exhibit the noisy fluctuation, non-monotonic change and abrupt increase near the end of life, all of which are less useful for the prognostics. On the other hand, the proposed energy entropy shows smooth and constant decrease over the cycle, which may be an indicator of the fault development. Many steps are remained for the feature to be valuable in the real field applications, and they are left as a future study.

ACKNOWLEDGEMENT

This paper was supported by Korea Agency for Infrastructure technology Advancement (KAIA) in 2016 (16RTRPB10437003000000)

REFERENCES

- An, D., Kim, N., & Choi, J. ., (2016). Bearing Prognostics Method Based on Entropy Decrease at Specific Frequency. In *18th AIAA Non-Deterministic Approaches Conference* (p. 1678).
- Caesarendra, W., Widodo, A., & Yang, B. S. (2010). Application of relevance vector machine and logistic regression for machine degradation assessment. *Mechanical Systems and Signal Processing*, 24(4), 1161-1171.
- FEMTO-ST, "IEEE PHM 2012 Data Challenge," online website, last accessed on May 31, 2012. <http://www.femto-st.fr/en/Researchdepartments/AS2M/Research-groups/PHM/IEEE-PHM-2012-Datachallenge.php>
- Heng, A., Zhang, S., Tan, A. C., & Mathew, J. (2009). Rotating machinery prognostics: State of the art, challenges and opportunities. *Mechanical systems and signal processing*, 23(3), 724-739.
- Jardine, A. K. (2006). *A review on machinery diagnostic and prognostics implementing condition-based maintenance*, *Mechanical systems and signal processing*
- Lee, J., Wu, F., Zhao, W., Ghaffari, M., Liao, L., & Siegel, D. (2014). Prognostics and health management design for rotary machinery systems—Reviews, methodology and applications. *Mechanical systems and signal processing*, 42(1), 314-334.
- Lebold, M., McClintic, K., Campbell, R., Byington, C., & Maynard, K. (2000, May). Review of vibration analysis methods for gearbox diagnostics and prognostics. In *Proceedings of the 54th Meeting of the Society for Machinery Failure Prevention Technology* (Vol. 634, p. 16).
- Lee, J., Qiu, H., Yu, G., & Lin, J. (2009). Rexnord Technical Services (2007). 'Bearing Data Set', IMS, University of Cincinnati. NASA Ames Prognostics Data Repository.
- McInerny, S. A., & Dai, Y. (2003). Basic vibration signal processing for bearing fault detection. *IEEE Transactions on education*, 46(1), 149-156.
- Qiu, H., Lee, J., Lin, J., & Yu, G. (2006). Wavelet filter-based weak signature detection method and its application on rolling element bearing prognostics. *Journal of sound and vibration*, 289(4), 1066-1090.
- Randall, R. B., & Antoni, J. (2011). Rolling element bearing diagnostics—a tutorial. *Mechanical Systems and Signal Processing*, 25(2), 485-520. ISO 690
- Siew, W. S., Smith, W. A., Peng, Z., & Randall, R. B. FAULT SEVERITY TRENDING IN ROLLING ELEMENT BEARINGS.
- Siegel, D., Ly, C., & Lee, J. (2011). Evaluation of vibration based health assessment and diagnostic techniques for helicopter bearing components. In *2011 DSTO International Conference on Health and Usage Monitoring, Melbourne, Australia*.
- Sutrisno, E., Oh, H., Vasan, A. S. S., & Pecht, M. (2012, June). Estimation of remaining useful life of ball bearings using data driven methodologies. In *Prognostics and Health Management (PHM), 2012 IEEE Conference on* (pp. 1-7). IEEE.
- Wang, T. (2012, June). Bearing life prediction based on vibration signals: A case study and lessons learned. In *Prognostics and Health Management (PHM), 2012 IEEE Conference on* (pp. 1-7). IEEE.
- Yan, W., Qiu, H., & Iyer, N. (2008). *Feature extraction for bearing prognostics and health management (phm)-a survey (preprint)* (No. AFRL-RX-WP-TP-2008-4309). AIR FORCE RESEARCH LAB WRIGHT-PATTERSON AFB OH MATERIALS AND MANUFACTURING DIRECTORATE.